Energy Minimization for UAV Enabled Video Relay System Under QoE Constraints

Han Hu[1(✉)], Cheng Zhan[2], and Jianping An[1]

[1] School of Information and Electronics, Beijing Institute of Technology, Beijing, China
{hhu,an}@bit.edu.cn
[2] School of Computer and Information Science, Southwest University, Chongqing, China
zhanc@swu.edu.cn

Abstract. With the explosive growth of mobile video services, unmanned aerial vehicle (UAV) is flexibly deployed as a relay node to offload cellular traffic or provide video services for emergency scenario without infrastructures. This paper proposes a novel design framework for UAV enabled video relay system with the aim of minimizing energy consumption of the UAV, subjecting to the QoE requirement of each GU. A dynamic resource allocation strategy is employed to model the UAV's power and bandwidth allocation and the optimization problem is formulated as a non-convex problem, via optimizing the transmit power and bandwidth allocation of the UAV jointly with the UAV trajectory. To tackle this non-convex problem, the original problem is decoupled into two sub-problems: bandwidth and transmit power allocation optimization, as well as UAV trajectory optimization. We propose an efficient iterative algorithm to obtain a Karush-Kuhn-Tucker (KKT) solution via solving the two sub-problems with successive convex approximation and alternating optimization techniques. Extensive simulations are conducted to evaluate the performance and the results demonstrate that with the proposed joint design, the UAV's energy consumption is significantly reduced, by up to 30%, and the QoE requirement for GUs can be well satisfied simultaneously.

Keywords: Unmanned aerial vehicle · Video relay system · Energy minimization · Quality of experience

1 Introduction

Recently, the global mobile data traffic has been dominated by mobile video streaming (e.g., Netflix and YouTube) [1], which is expected to grow due to the increasing use of higher resolution video formats e.g., 4K videos. On the other hand, the quality of experience (QoE) of end users will be degraded due

S. W. Loke et al. (Eds.): MONAMI 2020, LNICST 338, pp. 256–269, 2020.
https://doi.org/10.1007/978-3-030-64002-6_17

to the increased congestion brought by the growing popularity of video services, especially the cell edge users. As a result, recent researches have paid more attention on developing efficient solutions to meet the user's QoE requirement.

To tackle such issues, traditional solution is to deploy small-cell networks which consist of a large number of small base stations (SBSs). However, deploying a lot of fixed SBSs is cost-ineffective for scenarios with temporarily high user density or highly dynamic traffic demand [2]. Recently, unmanned aerial vehicles (UAVs) offer several opportunities for extending the coverage areas of current wireless networks, such as offloading overloaded traffic from existing cellular networks, or providing wireless video services as a relay node in infrastructure-less areas (e.g., due to disaster or maintenance), by relaying data from remote BSs [3]. Specifically, the channels between ground users (GUs) and the UAV have high probability to be line-of-sight (LoS) channels, where the transmission performance can be enhanced significantly [4]. Furthermore, since the UAV has high mobility, it is practical to deploy UAV flexibly and quickly for on-demand wireless systems, which is more suitable for the dynamic traffic demand scenario. In addition, the cost of deploying UAV is less expensive than that of deploying small-cell networks [5]. However, due to the flexible mobility of the UAV, the channel quality varies over time, which brings a great challenge to video services [6]. To tackle such challenge, dynamic adaptive video streaming over HTTP (DASH) is employed [7]. With DASH-based video streaming, the streaming media can dynamically select the most suitable video bitrate based on its instantaneous channel quality [8,9]. To be specific, DASH can adjust the video quality based on the available bandwidth or transmission rate between GUS and the UAV. This is a particularly useful feature for the UAV communication as the transmission rate of UAV-to-Ground (U2G) communication link may vary over time accordingly with time-varying channel quality. Average QoE was maximized for UAV-enabled DASH system in [9] by optimizing UAV's position and resource allocation without taking UAV's energy consumption into account.

Although DASH is adopted, new challenges arise for the UAV enabled video relay system. In particular, the UAV usually has very limited endurance since the onboard energy is limited, which requires to be efficiently utilized to prolong the UAV endurance. Compared to conventional terrestrial BSs, UAV flight (e.g., hovering or flying) incurs additional propulsion energy consumption. A fundamental tradeoff exists between maximizing QoE of GUs and minimizing UAV's energy consumption. Intuitively, if the UAV can fly closer to or even hover around each GU to provide video service with better channel quality, then the QoE of each GU increases. However, such trajectory leads to longer flying distance of the UAV, which will increase the UAV's energy consumption in general. It is difficult to achieve the optimal balance between maximizing QoE of GUs and minimizing UAV's energy consumption at the same time. Furthermore, the tradeoff between U2G channel quality and BS-to-UAV (B2U) channel quality for UAV relay platform should be investigated as the increment of U2G channel quality is generally at the cost of decrement of B2U channel quality. To provide energy efficient video services for GUs in UAV enabled relay system, the UAV's

energy consumption should be minimized while ensuring the QoE requirement of GUs, via optimizing bandwidth and transmit power allocation jointly with UAV trajectory. The main contributions of this paper is summarized as follows:

- Firstly, we propose a novel design framework for UAV enabled video relay system to provide video services. An optimization problem for the UAV enabled video relay system is formulated with the aim of minimizing the UAV's total energy consumption subjecting to the QoE constraints of GUs, via optimizing the bandwidth and transmit power allocation jointly with the UAV trajectory.
- Secondly, the formulated problem is a non-convex optimization problem and it is difficult to obtain optimal solution directly. We decompose the original problem into two sub-problems, i.e., transmit power and bandwidth allocation optimization, and UAV trajectory optimization, and an efficient iterative algorithm is proposed by employing successive convex approximation (SCA) and alternating optimization techniques, which converges to a Karush-Kuhn-Tucker (KKT) solution.
- Lastly, extensive simulations are conducted to evaluate the performance under different settings, and the results demonstrate that the proposed joint design can reduce the UAV's total energy consumption, up to 30%, over benchmark schemes, and the QoE requirement for GUs can be well satisfied simultaneously.

2 System Model and Problem Statement

2.1 System Model

We consider an area in which the established BS is not functioning (e.g., due to disaster or maintenance). Such area may be a remote area, where there is no direct links between other BSs and the GUs. There are M existing BSs and K GUs in such area, denoted by $\mathcal{S} = \{s_1, s_2, \ldots, s_M\}$ and $\mathcal{U} = \{u_1, u_2, \ldots, u_K\}$, respectively. We employ a rotary-wing UAV as a aerial relay platform to provide video services from existing BSs to multiple GUs since rotary-wing UAV can hover over GUs to provide better video services. All BSs are assumed to have the same altitude H_B, and we denote $\mathbf{s}_m$ and $\mathbf{w}_k$ as the horizontal locations of BS s_m and GU u_k, respectively. For simplicity, the UAV is assumed to fly at a constant altitude of H. The initial/final locations are pre-determined to be the same, which is given as $\mathbf{q}_I \in \mathbb{R}^{2\times 1}$. To facilitate the trajectory design of the UAV, the total time horizon is assumed to consist of $T > 0$ time slots, and δ_t is the time duration of the elemental time slot. Denote the horizonal location of UAV at time slot t as $\mathbf{q}[t] \in \mathbb{R}^{2\times 1}$, then the UAV's flying trajectory can be denoted as the discrete set $\{\mathbf{q}[t], 0 \le t \le T\}$. As a result, the UAV velocity in time slot t is calculated as $\mathbf{v}[t] \triangleq \frac{\mathbf{q}[t+1]-\mathbf{q}[t]}{\delta_t}$, $\|\mathbf{v}[t]\| \le V_{\max}, \forall t$, where $V_{\max}$ denotes the UAV's maximum speed.

The total bandwidth is denoted as B measured in hertz (Hz), and frequency division multiple access (FDMA) scheme is adopted by the UAV with dynamic bandwidth allocation among all BSs and GUs. In particular, at any time slot

of the UAV flight period, the UAV communicates with multiple BSs and GUs simultaneously by assigning each BS or GU a fraction of the total bandwidth. Let $x_m[t] \geq 0$ represent the allocated fraction of bandwidth to BS $s_m, 1 \leq m \leq M$ at time slot t, and let $y_k[t] \geq 0$ represent the allocated fraction of bandwidth to GU $u_k, 1 \leq k \leq K$. Thus, we have $\sum_{m=1}^{M} x_m[t] + \sum_{k=1}^{K} y_k[t] \leq 1, \forall t$.

2.2 Channel Model

For B2U communication, the channel between the UAV and each BS is dominated by the LoS link as in [5,10]. At time slot t, the distance between the mth BS and UAV is calculated as $\hat{d}_m[t] = \sqrt{(H - H_B)^2 + \|\mathbf{q}[t] - \mathbf{s}_m\|}$. The channel power gain between the UAV and s_m at time slot t is then written as $\hat{\beta}_m[t] = \beta_0 \hat{d}_m^{-2}[t]$, where β_0 is channel power gain at 1 meter. Let P_B be the transmit power for each BS. Denote $\hat{R}_m[t]$ as the normalized instantaneous achievable rate of BS s_m for B2U communication in time slot t measured in bits/second/Hz (bps/Hz), then $\hat{R}_m[t]$ is written as $\hat{R}_m[t] = x_m[t] \log_2 \left(1 + \frac{P_B \gamma_0}{x_m[t]((H-H_B)^2 + \|\mathbf{q}[t] - \mathbf{s}_m\|^2)}\right)$ where $\gamma_0 \triangleq \frac{\beta_0}{BN_0}$, with N_0 denoting the power spectral density of noise at the receiver.

For U2G communication, signal reflection and scattering occurs in air-to-ground communication links [4]. Denote $\check{h}_k[t]$ as channel coefficient at time slot t between GU u_k and the UAV, then $\check{h}_k[t] = \sqrt{\check{\beta}_k[t]}\check{\rho}_k[t]$, where $\check{\beta}_k[t]$ and $\check{\rho}_k[t]$ represent for the large-scale coefficient and small-scale fading coefficient, respectively. In particular, we have $\check{\beta}_k[t] = \beta_0 \check{d}_k^{-\alpha}[t]$, where $\alpha \geq 2$ denotes the path loss exponent. Denote $p_k[t] \geq 0$ as the UAV transmit power allocated to GU s_k in time slot t, then $\sum_{k=1}^{K} p_k[t] \leq P_U, \forall t$, where P_U is the UAV's maximum allowable transmit power. As such, the normalized instantaneous achievable rate of GU u_k for U2G communication at time slot t, denoted by $\check{R}_k[t]$, measured in bits/second/Hz (bps/Hz), is then expressed as $\check{R}_k[t] = y_k[t] \log_2 \left(1 + \frac{p_k[t]\gamma_0 |\check{\rho}_k[t]|^2}{y_k[t](H^2 + \|\mathbf{q}[t] - \mathbf{w}_k\|^2)^{\alpha/2}}\right)$. Note that $\check{R}_k[t]$ is a random variable since $\check{\rho}_k[t]$ is a random variable. To tackle such issue, we focus on the average rate similar as in [11], defined as $\mathbb{E}[\check{R}_k[t]]$, which is approximated as $\mathbb{E}[\check{R}_k[t]] \approx y_k[t] \log_2 \left(1 + \frac{p_k[t]\gamma_0}{y_k[t](H^2 + \|\mathbf{q}[t] - \mathbf{w}_k\|^2)^{\alpha/2}}\right) \triangleq \tilde{R}_k[t]$, where $\tilde{R}_k[t]$ can be interpreted as an approximation of the average rate $\mathbb{E}[\check{R}_k[t]]$. It is shown in [11] that high accuracy can be achieved for such approximation, especially for rural or suburban environment.

2.3 Video Streaming and Energy Consumption Model

We consider a video-on-demand scenario. K GUs request for different video contents from BSs via the relay of UAV. The UAV fetches video contents from M BSs, and then forwards packets to K GUs. At each time slot t, the UAV can only relay the video data which has already been received from BSs. Thus, we have the following information-causality constraint by assuming that the processing delay

at the UAV is one slot [5], i.e., $\sum_{n=0}^{t-1}\sum_{m=1}^{M}\hat{R}_m[n] \geq \sum_{n=1}^{t}\sum_{k=1}^{K}\tilde{R}_k[n], t = 1, 2, \ldots, T$.

We assume that the UAV enabled video relay system employs DASH for video streaming, which can dynamically adapt the video rate based on channel conditions. For simplicity, similar as in [12], the QoE (i.e. the utility) of users is modelled as a logarithmic function with transmission rate. In particular, the QoE utility of GU u_k is expressed as $\theta \log \beta \frac{\bar{R}_k}{r_k}$, where θ and β are positive constants which are different for various types of applications, and $\bar{R}_k \triangleq \frac{1}{T}\sum_{t=1}^{T}\tilde{R}_k[t]$ denotes the time-averaged transmission rate for GU u_k. r_k denotes the required playback rate for GU u_k, which depends on the physical capability of media outlet. As a result, we have $\theta \log \frac{\beta \sum_{t=1}^{T}\tilde{R}_k[t]}{T r_k} \geq U_k, \forall k$, where U_k represents the minimum QoE utility for GU u_k.

Typically, the UAV's energy consumption consists of both communication related energy consumption and propulsion energy consumption. The communication related energy consumption of the UAV can be calculated as $E_c(\{p_k[t]\}) \triangleq \sum_{k=1}^{K}\sum_{t=1}^{T}\delta_t p_k[t]$. On the other hand, the propulsion energy consumption of rotary-wing UAV was given in [11], i.e.,

$$E_p(\{\mathbf{v}[t]\}) \approx \sum_{t=1}^{T}\delta_t\left(P_0 + \frac{3P_0\left\|\mathbf{v}[t]\right\|^2}{U_{tip}^2} + \frac{1}{2}d_0\rho s A\left\|\mathbf{v}[t]\right\|^3\right) + \sum_{t=1}^{T}\delta_t P_i\left(\sqrt{1+\frac{\left\|\mathbf{v}[t]\right\|^4}{4v_0^4}} - \frac{\left\|\mathbf{v}[t]\right\|^2}{2v_0^2}\right)^{\frac{1}{2}}, \tag{1}$$

where constants P_i and P_0 denote the hovering related induced power and blade profile, respectively. U_{tip} and v_0 denote the tip speed of rotor blade and mean rotor induced velocity when hovering. d_0 and s denote the fuselage drag ratio and rotor solidity. The air density and rotor disc area are denoted as ρ and A, respectively.

2.4 Problem Formulation

In this paper, our goal is to minimize the UAV's total energy consumption during a continuous period of T time slots, while ensuring that the target QoE utility for each GU is achieved, by jointly optimizing the UAV trajectory $\mathcal{Q} \triangleq \{\mathbf{q}[t]\}$ and bandwidth allocations $\mathcal{B} \triangleq \{x_m[t], y_k[t]\}$, as well as transmit power allocation $\mathcal{P} \triangleq \{p_k[t]\}$. Based on the various models derived above, the optimization problem can be expressed as follows:

$$(\text{P1}): \min_{\mathcal{Q},\mathcal{B},\mathcal{P}} \ E_c(\{p_k[t]\}) + E_p(\{\mathbf{v}[t]\})$$

$$\text{s.t.} \ \ \theta \log \frac{\beta \sum_{t=1}^{T} \tilde{R}_k[t]}{T r_k} \geq U_k, \forall k, \tag{2}$$

$$\sum_{n=0}^{t-1} \sum_{m=1}^{M} \hat{R}_m[n] \geq \sum_{n=1}^{t} \sum_{k=1}^{K} \tilde{R}_k[n], t = 1, \ldots, T, \tag{3}$$

$$\sum_{m=1}^{M} x_m[t] + \sum_{k=1}^{K} y_k[t] \leq 1, \forall t, \tag{4}$$

$$x_m[t] \geq 0, y_k[t] \geq 0, \forall m, k, t, \tag{5}$$

$$\sum_{k=1}^{K} p_k[t] \leq P_U, \forall t, \tag{6}$$

$$\|\mathbf{v}[t]\| \leq V_{\max}, \forall t, \tag{7}$$

$$\mathbf{q}[0] = \mathbf{q}_I, \mathbf{q}[T] = \mathbf{q}_I. \tag{8}$$

In (P1), constraints in (2) impose a minimum QoE utility U_k for each GU u_k. Constraints in (3) are the information-causality constraints. Constraints in (4) and (5) are imposed due to dynamic bandwidth allocation scheme among all BSs and GUs. Constraints in (6)-(8) represent the UAV's physical constraints. Note that problem (P1) is non-convex which consists of coupled variables, and it is difficult to obtain the optimal solution of (P1) directly. In the following section, an effective method is proposed to obtain a sub-optimal solution to (P1) by iteratively solving its two sub-problems.

3 Proposed Solution

3.1 Bandwidth and Transmit Power Allocation

In this subsection, we consider the bandwidth and transmit power allocation with given UAV trajectory $\mathcal{Q}$. The UAV's propulsion energy consumption, i.e., E_p, is fixed due to the fixed trajectory $\mathcal{Q}$, and then problem (P1) reduces to:

$$(\text{P2}): \min_{\mathcal{B},\mathcal{P}} \ E_c(\{p_k[t]\}) + E_p$$
$$\text{s.t.} \ \ (2) - (6).$$

Although UAV trajectory $\mathcal{Q}$ is given, problem (P2) remains non-convex since constraints (2) and (3) are still non-convex constraints. By employing the slack variables $\mathcal{W} \triangleq \{\omega_k[t], \forall k, t\}$, (P2) can be reformulated as

$$\text{(P3)}: \min_{\mathcal{B},\mathcal{P},\mathcal{W}} \; E_c(\{p_k[t]\}) + E_p$$
$$\text{s.t.} \; (4)-(6),$$
$$\theta \log \frac{\beta \sum_{t=1}^{T} \omega_k[t]}{Tr_k} \geq U_k, \forall k, \tag{9}$$
$$y_k[t] \log_2 \left(1 + \frac{p_k[t]\gamma_0}{y_k[t](H^2 + \|\mathbf{q}[t] - \mathbf{w}_k\|^2)^{\alpha/2}}\right) \geq \omega_k[t], \quad \forall k, t, \tag{10}$$
$$\sum_{n=0}^{t-1} \sum_{m=1}^{M} x_m[n] \log_2 \left(1 + \frac{P_B \gamma_0}{x_m[n]((H - H_B)^2 + \|\mathbf{q}[n] - \mathbf{s}_m\|^2)}\right) \geq \sum_{n=1}^{t} \sum_{k=1}^{K} \omega_k[n], t = 1, \ldots, T. \tag{11}$$

Theorem 1. *Problem (P3) is equivalent to problem (P2).*

Proof. Considering problem (P3), it can be shown that in the optimal solution to (P3), equality holds in all constraints of (10), i.e., $\tilde{R}_k[t] = \omega_k[t], \forall k, t$. Since otherwise, we can decrease $p_k[t]$ to satisfy the equality, then the objective value of (P3) can be further reduced since E_c decreases while E_p keeps the same, and all other constraints are still satisfied. Therefore, in the optimal solution to problem (P3), $\tilde{R}_k[t] = \omega_k[t], \forall k, t$. By substituting $\omega_k[t]$ with $\tilde{R}_k[t]$ in (9) and (11), problem (P3) is the same as problem (P2), and the proof concludes. □

Note (P3) is a standard convex optimization problem, where standard convex optimization techniques or existing solvers such as CVX[13] can be leveraged to solve (P3) efficiently.

3.2 UAV Trajectory Optimization

In this subsection, we focus on solving the sub-problem of UAV trajectory optimization problem with given bandwidth and transmit power allocation. As such, UAV's communication-related energy consumption, i.e., E_c, is fixed. This sub-problem is written as:

$$\text{(P4)}: \min_{\mathcal{Q},\mathcal{V},\mathcal{W}} \; E_c + E_p(\{\mathbf{v}[t]\})$$
$$\text{s.t.} \; \theta \log \frac{\beta \sum_{t=1}^{T} \omega_k[t]}{Tr_k} \geq U_k, \forall k, \tag{12}$$
$$y_k[t] \log_2 \left(1 + \frac{p_k[t]\gamma_0}{y_k[t](H^2 + \|\mathbf{q}[t] - \mathbf{w}_k\|^2)^{\alpha/2}}\right) \geq \omega_k[t], \quad \forall k, t, \tag{13}$$
$$\sum_{n=0}^{t-1} \sum_{m=1}^{M} x_m[n] \log_2 \left(1 + \frac{P_B \gamma_0}{x_m[n]((H - H_B)^2 + \|\mathbf{q}[n] - \mathbf{s}_m\|^2)}\right)$$

$$\geq \sum_{n=1}^{t}\sum_{k=1}^{K}\omega_k[n], t = 1, \ldots, T. \tag{14}$$

$$(7), (8),$$

Problem (P4) is non-convex due to the non-convex objective function and both constraints (13) and (14) contain non-convex constraints. To tackle the non-convex term in $E_p(\{\mathbf{v}[t]\})$, slack variables $\mathcal{T} \triangleq \{\tau[t] \geq 0\}$ is introduced such that $\tau[t] = \left(\sqrt{1 + \frac{\|\mathbf{v}[t]\|^4}{4v_0^4}} - \frac{\|\mathbf{v}[t]\|^2}{2v_0^2}\right)^{1/2}$, and then we obtain $\frac{1}{\tau[t]^2} = \tau[t]^2 + \frac{\|\mathbf{v}[t]\|^2}{v_0^2}$. Define $E_p^\tau(\{\mathbf{v}[t]\}, \{\tau[t]\}) \triangleq \sum_{t=1}^{T} \delta_t \left(P_0 + \frac{3P_0\|\mathbf{v}[t]\|^2}{U_{tip}^2} + \frac{1}{2}d_0\rho s A \|\mathbf{v}[t]\|^3 + P_i\tau[t]\right)$, where $E_p^\tau(\{\mathbf{v}[t]\}, \{\tau[t]\})$ is joint convex with $\{\mathbf{v}[t]\}$ and $\{\tau[t]\}$, then (P4) is reduced to

$$\begin{aligned}(\text{P5}): \min_{\mathcal{Q},\mathcal{V},\mathcal{W},\mathcal{T}} \quad & E_c + E_p^\tau(\{\mathbf{v}[t]\}, \{\tau[t]\}) \\ \text{s.t.} \quad & \tau[t]^2 + \frac{\|\mathbf{v}[t]\|^2}{v_0^2} = \frac{1}{\tau[t]^2}, \forall t, \\ & (7), (8), (12) - (14).\end{aligned} \tag{15}$$

Note that problem (P5) remains non-convex since non-affine equality constraint exists in (15). To tackle such difficulty, we relax the equality constraint into the following inequality constraint, i.e.,

$$\begin{aligned}(\text{P6}): \min_{\mathcal{Q},\mathcal{V},\mathcal{W},\mathcal{T}} \quad & E_c + E_p^\tau(\{\mathbf{v}[t]\}, \{\tau[t]\}) \\ \text{s.t.} \quad & \tau[t]^2 + \frac{\|\mathbf{v}[t]\|^2}{v_0^2} \geq \frac{1}{\tau[t]^2}, \forall t, \\ & (7), (8), (12) - (14).\end{aligned} \tag{16}$$

Similar as that in Theorem 1, it is not difficult to see that at the optimal solution to (P6), equality holds in (16). Since otherwise, $\tau[t]$ can always be decreased until the equality is met, and the objective value will decrease since $E_p^\tau(\{\mathbf{v}[t]\}, \{\tau[t]\})$ is a monotonic increasing function with respect to $\tau[t]$. Therefore, solving problem (P5) is equivalent to solving problem (P6).

However, problem (P6) is still non-convex since non-convex constraints exist in (13), (14) and (16). To address such challenges, SCA technique is utilized to derive their convex approximations. Specifically, it can be shown that the first-order Taylor approximation of a convex function can be regarded as a global under-estimator [14], and $\tilde{R}_k[t]$ is convex with respect to term $\|\mathbf{q}[t] - \mathbf{w}_k\|^2$, then $\tilde{R}_k[t]$ can be lower-bounded at the given point $\mathbf{q}^r[t]$, as in [5,10,15], i.e.,

$$\begin{aligned}\tilde{R}_k[t] \; & \geq y_k[t](A_k^r[t] - I_k^r[t](\|\mathbf{q}[t] - \mathbf{w}_k\|^2 - \|\mathbf{q}^r[t] - \mathbf{w}_k\|^2)) \\ & \triangleq \tilde{R}_k^{lb}[t]\end{aligned} \tag{17}$$

where $I_k^r[t] = \frac{(\alpha/2)p_k[t]\gamma_0 \log_2 e}{(H^2+\|\mathbf{q}^r[t]-\mathbf{w}_k\|^2)(y_k[t](H^2+\|\mathbf{q}^r[t]-\mathbf{w}_k\|^2)^{\alpha/2}+p_k[t]\gamma_0)}$ and $A_k^r[t] = \log_2\left(1+\frac{p_k[t]\gamma_0}{y_k[t](H^2+\|\mathbf{q}^r[t]-\mathbf{w}_k\|^2)^{\alpha/2}}\right)$. The equality of (17) holds at the point $\mathbf{q}[t] = \mathbf{q}^r[t]$ and both $\tilde{R}_k[t]$ and $\tilde{R}_k^{lb}[t]$ have identical gradient, i.e., $\nabla\tilde{R}_k[t] = \nabla\tilde{R}_k^{lb}[t], \forall k, t$.

Similarly, $\hat{R}_m[t]$ is lower-bounded as follows:

$$\begin{aligned}\hat{R}_m[t] &\geq x_m[t](\hat{A}_m^r[t] - \hat{I}_m^r[t](\|\mathbf{q}[t]-\mathbf{s}_m\|^2 - \|\mathbf{q}^r[t]-\mathbf{s}_m\|^2)) \\ &\triangleq \hat{R}_m^{lb}[t] \end{aligned} \tag{18}$$

where $\hat{A}_m^r[t] = \log_2\left(1+\frac{P_B\gamma_0}{x_k[t]((H-H_B)^2+\|\mathbf{q}^r[t]-\mathbf{s}_m\|^2)}\right)$, $\hat{I}_m^r[t] = \frac{P_B\gamma_0 \log_2 e}{\hat{J}_m^r[t]\left(x_k[t]\hat{J}_m^r[t]+P_B\gamma_0\right)}$, and $\hat{J}_m^r[t] = (H-H_B)^2 + \|\mathbf{q}^r[t]-\mathbf{s}_m\|^2$.

On the other hand, since terms $\|\mathbf{v}[t]\|^2$ and $\tau[t]^2$ are convex with $\mathbf{v}[t]$ and $\tau[t]$, respectively. By applying first-order Taylor expansion at local points $\mathbf{v}^r[t]$ and $\tau^r[t]$, we have

$$\|\mathbf{v}[t]\|^2 \geq \|\mathbf{v}^r[t]\|^2 + 2(\mathbf{v}^r[t])^T(\mathbf{v}[t]-\mathbf{v}^r[t]) \triangleq z_v^{lb}[t], \forall t, \tag{19}$$

$$\tau[t]^2 \geq (\tau^r[t])^2 + 2\tau^r[t](\tau[t]-\tau^r[t]) \triangleq z_\tau^{lb}[t], \forall t. \tag{20}$$

By substituting (17) and (18) into the left-hand sides(LHSs) of (13) and (14), respectively, and substituting (19) and (20) into the LHSs of (16), problem (P6) can be approximated as follows:

$$\begin{aligned}(\text{P7}): \min_{\mathcal{Q},\mathcal{V},\mathcal{W},\mathcal{T}} \; & E_c + E_p^\tau(\{\mathbf{v}[t]\},\{\tau[t]\}) \\ \text{s.t.} \; & z_\tau^{lb}[t] + \frac{z_v^{lb}[t]}{v_0^2} - \frac{1}{\tau[t]^2} \geq 0, \forall t, && (21) \\ & \tilde{R}_k^{lb}[t] \geq \omega_k[t], \forall k, t, && (22) \\ & \sum_{n=0}^{t-1}\sum_{m=1}^{M}\hat{R}_m^{lb}[n] \geq \sum_{n=1}^{t}\sum_{k=1}^{K}\omega_k[n], t = 1,\ldots,T, \\ & (7),(8),(12). && (23)\end{aligned}$$

Note that problem (P7) is now convex, and then CVX solvers and be utilized to solve (P7) efficiently.

3.3 Overall Iterative Algorithm, Convergence, and Complexity

Using the results obtained above, we propose an overall algorithm for computing the suboptimal solution to (P1) by employing SCA and alternating optimization techniques, where we summarize the details in Algorithm 1.

Algorithm 1. Iterative Bandwidth and Transmit Power Allocation, and Trajectory Optimization Algorithm for (P1)

1: Initialize $\mathcal{Q}^0$. Let $r \leftarrow 0$.
2: **repeat**
3: Solve convex problem (P3) with CVX to obtain $\mathcal{B}^{r+1}$ and $\mathcal{P}^{r+1}$ with given $\mathcal{Q}^r$;
4: Solve convex problem (P7) with CVX to obtain $\mathcal{Q}^{r+1}$ with given $\mathcal{B}^{r+1}$ and $\mathcal{P}^{r+1}$, as well as $\mathcal{Q}^r$;
5: $r \leftarrow r + 1$;
6: **until** The objective value of (P1) converges

Theorem 2. *The proposed Algorithm 1 is convergent.*

Proof. Denote $E(\mathcal{B}^r, \mathcal{P}^r, \mathcal{Q}^r)$ as the objective value of problem (P1) in the rth iteration. Recall that the optimal solution $\mathcal{P}^{r+1}, \mathcal{B}^{r+1}$ is obtained by solving convex problem (P3), we have $E(\mathcal{B}^r, \mathcal{P}^r, \mathcal{Q}^r) \geq E(\mathcal{B}^{r+1}, \mathcal{P}^{r+1}, \mathcal{Q}^r)$. Denote E^{up} as the objective value of problem (P7), we have

$$\begin{aligned} &E(\mathcal{B}^{r+1}, \mathcal{P}^{r+1}, \mathcal{Q}^r) \overset{(a)}{=} E^{up}(\mathcal{B}^{r+1}, \mathcal{P}^{r+1}, \mathcal{Q}^r) \\ &\overset{(b)}{\geq} E^{up}(\mathcal{B}^{r+1}, \mathcal{P}^{r+1}, \mathcal{Q}^{r+1}) \overset{(c)}{\geq} E(\mathcal{B}^{r+1}, \mathcal{P}^{r+1}, \mathcal{Q}^{r+1}). \end{aligned} \tag{24}$$

Recall that first-order Taylor expansions at given local points are tight in problem (P6), then (a) holds. (b) holds due to the fact that problem (P7) is optimally solved. Recall that the objective value of (P7) is an upper bound of that to (P6), then the inequality of (c) holds. As a result, we have $E(\mathcal{B}^r, \mathcal{P}^r, \mathcal{Q}^r) \geq E(\mathcal{B}^{r+1}, \mathcal{P}^{r+1}, \mathcal{Q}^{r+1})$. Therefore, the objective value of (P1) is non-increasing over iterations, which is lower bounded by a finite value. Furthermore, the first-order Taylor expansions have identical gradients as original functions. Therefore, Algorithm 1 converges to a KKT solution [5], i.e. the proposed Algorithm is convergent.

Note that Algorithm 1 requires alternatively solving problems (P3) and (P7), which are both standard convex optimization problems. Therefore, given the prescribed accuracy κ and let L be the number of iterations before convergence, then the computational complexity of Algorithm 1 is given by $O(LM^3K^3T^3)$[14], and L is in the order of $\log \frac{1}{\kappa}$.

4 Simulation Results

We consider a UAV enabled video relay system, which consists of $M = 2$ existing BSs and $K = 5$ GUs. The GUs are randomly located in a square area of 1.0×1.0 km^2, and the two BSs are located at the left/right side of this area, i.e., $\mathbf{s}_1 = [-500, 0]^T, \mathbf{s}_2 = [500, 0]^T$. $\mathbf{q}_I$ is set to be $[-200, 100]^T$. For the utility parameters, we set $r_k = 1$ Mbps, $\forall k$, and $\theta = 0.8$, similar to that in [12]. Furthermore, all GUs are assumed to have identical QoE requirements, i.e., $U_k = \bar{U}, \forall k$. In

addition, similar as in [11], the rotary-wing UAV's propulsion energy parameters are set as $d_0 = 0.6, U_{tip} = 120, A = 0.503, \rho = 1.225, s = 0.05, v_0 = 4.03, P_0 = 79.8563, P_i = 88.6279$. We set $H = 100$ m, $H_s = 50$ m, $V_{\max} = 30$ m/s, $P_B = 1$ W, $P_U = 0.1$ W, $B = 1$ MHz, $\delta_t = 1$ s, $\alpha = 2.2$, $N_0 = -170$ dBm/Hz, $\beta_0 = -60$ dB.

The optimized trajectory under different QoE requirement $\bar{U}$ are shown in Fig. 1(a) with $T = 120$. It can be seen that with the increase of QoE requirement $\bar{U}$, the UAV can adjust its trajectory to move close to the BSs to obtain more video data, and then move closer to or even hover over GUs to provide better video service, as expected. When $\bar{U}$ decreases, the UAV trajectory shrinks and mainly consists of smooth curves. The reason is that the UAV does not have to move close to the BSs and GUs with low $\bar{U}$. Such trajectory will result in less energy consumption of the UAV since the smaller flying distance is needed to serve all GUs, and UAV's propulsion energy consumption achieves the smallest value with UAV speed around 12 m/s due to (1). This trend can also be observed in Fig. 1(b). If the QoE requirement $\bar{U}$ is sufficiently large, the UAV tends to fly over each BS and GU with the maximum speed. The reason is that the UAV should fly close to the BSs and GUs so that better communication channel are achieved for satisfying large QoE requirement.

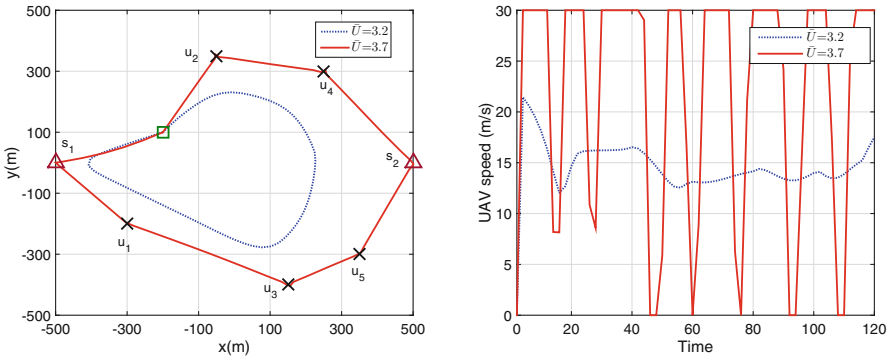

(a) Optimized trajectory (b) UAV speed

Fig. 1. Optimized trajectories and UAV speed with different QoE requirement $\bar{U}$. The square denotes the initial and final UAV locations, and the triangles denote different existing BSs.

Figure 2 reflects the bandwidth and transmit power allocation with $T = 120, \bar{U} = 3.2$. From Fig. 2(a), it can be seen that the UAV only relays video data when the UAV flies sufficiently close to the corresponding GU. The UAV's transmit power is small since the QoE requirement for GUs $\bar{U}$ is small. The bandwidth allocation over each time slot for all GUs and BSs is shown in Fig. 2(b). The bandwidth is allocated to the BS if the UAV moves close to it such that more video data can be obtained. Such bandwidth allocation for all BSs is enough

for each GU to achieve its QoE requirement. This is expected since the UAV relay's position can be dynamically adjusted to enhance the B2U and U2G links, respectively.

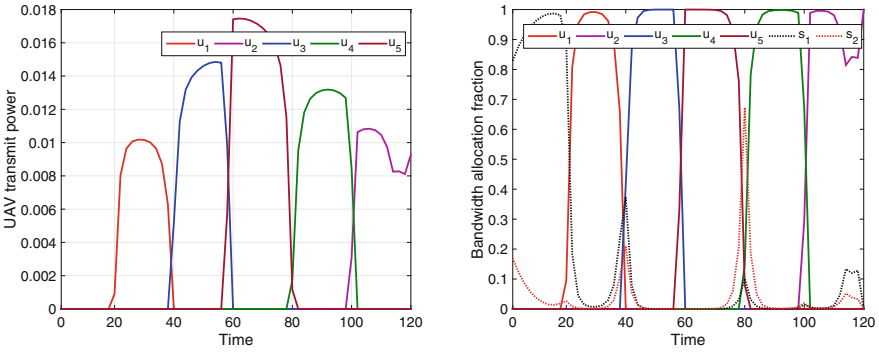

(a) UAV transmit power allocation among all GUs.

(b) Bandwidth allocation among all GUs and BSs.

Fig. 2. Bandwidth and transmit power with $T = 120, \bar{U} = 3.2$.

Finally, we compare the UAV's total energy consumption between our proposed scheme and three benchmark schemes, which are referred to *Static relaying benchmark* and *TSP benchmark*, as well as *QoE maximum benchmark*. In the static relaying benchmark, the UAV hovers over $\mathbf{q}_I$ all the time, and the resource allocation is optimized by solving (P2) with convex optimization technique. In the TSP benchmark, the UAV flies by following the TSP path to visit all GUs and BSs with maximum speed, and the resource allocation is optimized by solving (P2), similar as [16]. In the QoE maximum benchmark, the bandwidth and transmit power allocation are optimized jointly with UAV trajectory to maximize the minimum QoE among all GUs, similar as [10]. From Fig. 3, we can see that our proposed schemes can achieve lower energy consumption of the UAV than other benchmarks, and the gain are brought from the joint design of resource allocation and UAV trajectory.

In Fig. 3(a), it can be seen that the UAV's total energy consumption increases as T increases when $\bar{U} = 3.2$, and the achieved gain is remarkable with larger T. This is because the UAV's flying distance generally increases as T increases. When T is large enough, the UAV can hover over each BS to obtain more video data and hover above each GU in order to provide better video service. Figure 3(b) shows the impact of the QoE requirement $\bar{U}$ with different schemes when $T = 120$. The UAV's energy consumption increases when $\bar{U}$ increases since the UAV needs to to hover around each GU in order to provide better video service, which shows the trade off between minimizing the UAV's energy consumption and maximizing the QoE requirement. It is also observed that static relaying benchmark is not able to support larger QoE requirement, where such

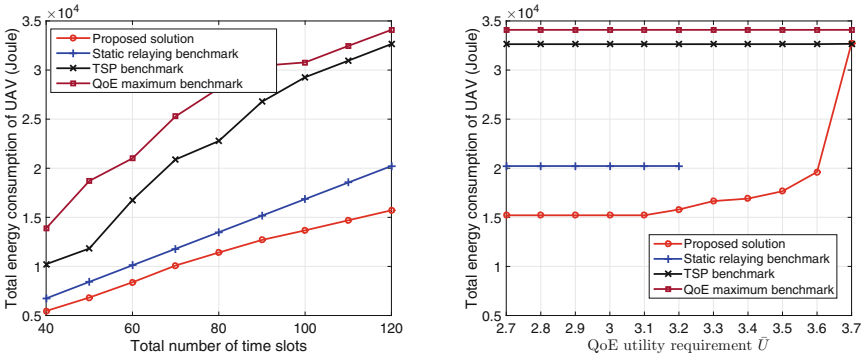

(a) Total energy consumption of the UAV versus T ($\bar{U} = 3.2$)

(b) Total energy consumption of the UAV versus $\bar{U}$ ($T = 120$)

Fig. 3. Total energy consumption of the UAV versus T or $\bar{U}$.

points do not appear in the figure. Furthermore, the performance of the three benchmarks varies a little. The reason is that the UAV trajectory is fixed, and the fixed propulsion energy dominates the UAV's energy consumption.

5 Conclusion

This paper considers a novel UAV enabled video relay system with a UAV relaying video data from multiple BSs to multiple GUs. The aim is to minimize the UAV's energy consumption of while guaranteeing the QoE constraint of each GU, via optimizing the bandwidth and transmit power allocation jointly with UAV trajectory. We propose an efficient iterative algorithm to obtain a KKT solution by using alternating optimization and SCA techniques, and the performance is evaluated numerically as compared to other benchmarks. The proposed design framework is general and can be applied to joint design resource allocation and UAV trajectory in other UAV enabled video streaming systems.

Acknowledgement. This work was supported by the National Natural Science Foundation of China under No. 61702426 and No. 61971457, Fundamental Research Funds for the Central Universities under Grant XDJK2019C084.

References

1. Cisco company: Visual networking index: Global mobile data traffic forecast update, 2016–2021 (2017)
2. Lyu, J., Zeng, Y., Zhang, R.: UAV-aided offloading for cellular hotspot. IEEE Trans. Wireless Commun. **17**(6), 3988–4001 (2018)
3. Chen, Y., Zhao, N., Ding, Z., Alouini, M.: Multiple UAVs as relays: multi-hop single link versus multiple dual-hop links. IEEE Trans. Wireless Commun. **17**(9), 6348–6359 (2018)

4. Khuwaja, A.A., Chen, Y., Zhao, N., Alouini, M.-S., Dobbins, P.: A survey of channel modeling for UAV communications. IEEE Commun. Surv. Tutor. **20**(4), 2804–2821 (2018)
5. Zeng, Y., Zhang, R., Lim, T.J.: Throughput maximization for UAV-enabled mobile relaying systems. IEEE Trans. Commun. **64**(12), 4983–4996 (2016)
6. She, C., Liu, C., Quek, T.Q.S., Yang, C., Li, Y.: Ultra-reliable and low-latency communications in unmanned aerial vehicle communication systems. IEEE Trans. Commun. **67**(5), 3768–3781 (2019)
7. Jiang, Z., Xu, C., Guan, J., Liu, Y., Muntean, G.: Stochastic analysis of DASH-based video service in high-speed railway networks. IEEE Trans. Multimedia **21**(6), 1577–1592 (2019)
8. Gao, G., et al.: Optimizing quality of experience for adaptive bitrate streaming via viewer interest inference. IEEE Trans. Multimedia **20**(12), 3399–3413 (2018)
9. Hu, H., Zhan, C., An, J., Wen, Y.: Optimization for HTTP adaptive video streaming in UAV-enabled relaying system. In: Proceedings of IEEE ICC, Shanghai, China, pp. 1–6 (2019)
10. Wu, Q., Zhang, R.: Common throughput maximization in UAV-enabled OFDMA systems with delay consideration. IEEE Trans. Commun. **66**(12), 6614–6627 (2018)
11. Zeng, Y., Xu, J., Zhang, R.: Energy minimization for wireless communication with rotary-wing UAV. IEEE Trans. Wireless Commun. **18**(4), 2329–2345 (2019)
12. Zhang, W., Wen, Y., Chen, Z., Khisti, A.: QoE-driven cache management for HTTP adaptive bit rate streaming over wireless networks. IEEE Trans. Multimedia **15**(6), 1431–1445 (2013)
13. Grant, M., Boyd, S.: CVX: MATLAB Software for Disciplined Convex Programming. http://cvxr.com/cvx
14. Boyd, S., Vandenberghe, L.: Convex Optimization. Cambridge University Press, Cambridge (2004)
15. Zhan, C., Zeng, Y., Zhang, R.: Energy-efficient data collection in UAV enabled wireless sensor network. IEEE Wirel. Commun. Lett. **7**(3), 328–331 (2018)
16. Zhang, J., Zeng, Y., Zhang, R.: UAV-enabled radio access network: multi-mode communication and trajectory design. IEEE Trans. Signal Process. **66**(20), 5269–5284 (2018)